City Research Online

City, University of London Institutional Repository

This is the accepted version of the paper.

This version of the publication may differ from the final published version.

Axial Compressive capacity of RC Square Columns strengthened by Prestressed CFRP with RPC pads

Qiang Wang [1,2,3], Chunling lu [1,3],   Wanxu Zhu [1,3]   Feng Fu[4]*, Kai Qian[1]

1 College of Civil and Architecture Engineering, Guilin University of Technology, Guilin 541004, China.

2 Guangxi Key Laboratory of New Energy and Building Energy Saving, Guilin 541004, China.

3 Guilin University of Technology, Collaborative Innovation Center for Exploration of Hidden Nonferrous Metal Deposits and Development of New Materials in Guangxi, Guilin 541004, China.

4. School of Mathematics, Computer Science and Engineering, City, University of London, London EC1C,0HB U.K.

Abstract: In this paper, a new technique to strengthen RC square columns using prestressed CFRP patched by ractive powder concrete (RPC) pad is developed. Fifteen RC square columns strengthened using this new technique were tested under axial compression loads. The influence of the level of prestress force, the number of wrapping layers and the strengthening process on the strengthening effect of this new technique was investigated. The improvement of compressive capacities and failure modes of the columns were studied. The results show that: this new technique provides better strengthening to the concrete columns with a fast strengthening process. The axial compression capacity of RC columns increases up to 80%. It is also found that, increasing the prestress can also improve the performance of the columns under normal working condition. A formula to predict the axial compression capacity of the columns is developed in this paper, which can accurately predict the axial compressive strength of the concrete columns strengthened by this new technique.

Key words: Fiber reinforced polymer; RPC pad; prestressed CFRP; strengthened; RC square columns; axial compressive capacity

---

* Corresponding author: E-mail address: cenffu@yahoo.co.uk

1. Introduction

The compressive failure of concrete starts with the development of internal cracks, However, confined concrete can limit the development of internal cracks, therefore, the axial compressive strength and ductility of concrete can be improved [1-3]. Fiber reinforced composite (FRP) has excellent properties such as light weight, high strength and corrosion resistance. In recent years, especially after the Northridge earthquake in the United States and the Hanshin earthquake in Japan, the technology of strengthening concrete structure using FRP retrofitting techniques has been well developed [4-8]. Among them, the most popular FRP used in the retrofitting projects is carbon fiber reinforced composite (CFRP), due to its high tensile strength, excellent strengthening effect. The pertinent technical specifications [9] are also developed. The research shows that the bearing capacity and ductility of concrete columns can be significantly improved by strengthening them using CFRP [10-14]. However, this traditional adhesive strengthening technology has some technical defects, such as low efficient usage of the fiber cloth, easy aging of structural adhesive and peeling off of the cloth [15]. Only 20 to 30% of the strength of carbon-fiber-reinforced polymer (CFRP) strips is used when they are applied as externally bonded strips for flexural and shear strengthening or in confinement of reinforced concrete (RC) structural elements. The research of [16][17], noticed that, when CFRP material is prestressed, the CFRP's strength can be further explored. This type of CFRP trips offers several advantages, including reduced crack widths, reduced deflections, reduced stress in the internal steel, and possibly increased fatigue resistance. To tackle this problem, applying prestressed force can fully utilized the strength of the FRP cloth, in the meantime, the lag problem of CFRP can be alleviated. Therefore, the performance of the compression column can be significantly improved [18]. However, at present, prestressed CFRP reinforced concrete columns still have the following problems: 1. in real construction projects, the concrete columns are in a loaded state, and the material already has initial stress or plastic deformation. The need to be further studied. 2. When the column section is rectangular, in order to avoid the stress concentration of the column angle, the traditional construction process is to grind it into a round corner, but this method will not only damage the original structure, but also cause low construction efficiency and dust pollution, further design improvements are needed. 3, CFRP is a fabric, it is not easy to apply large prestress (the maximum degree of prestress given in [19] is only 0.25), but the value can be improved by optimizing the strengthening process. 4. When the component is under high prestress, the pressure performance is yet to be studied.

Reactive powder concrete (RPC) is an ultra-high-performance cement-based composite material with much higher strength than ordinary concrete [20]. The density, elastic modulus and Poisson's ratio of RPC are close to that of ordinary concrete. When they are bonded with normal concrete, the deformation is similar, and there is no relative slip. At the same time, there is no coarse aggregate used in RPC but steel fiber, which has higher resistance. Tensile strength, toughness and durability of RPC are just suitable as a force transmission medium between the CFRPs and the concrete structural members, It can be prefabricated by modularized RPC blocks (the rounded corner can be prefabricated, avoiding manual grinding on site), therefore, they can be

attached to the outer surface of the column as a pad to transfer the "binding force" of the prestressed CFRP.

In terms of the analytical model of confined concrete, Mander J. B [21] established a stress-strain model for steel confined concrete in 1988, which was also used in FRP confined concrete in the early stage. However, it was found because these models can not reflect the real characteristics of FRP confined concrete, it is not suitable to apply them to FRP confined concrete. Lam L. and Teng J. g. [22] proposed a particular stress-strain model for FRP confined concrete and validated with experimental data. In the calculation of axial bearing capacity of confined concrete columns under load, Zhao et al. [23], Huang et al. [24], Pan et al. [25] all use the concept of "residual strength", that is, the strengthening effect under load is only effective for the residual stress of the core concrete, but invalid for the stress generated by the core concrete itself under initial load. Using the superposition of two-stage, the calculation model of the axialcapacity of concrete columns strengthened with FRP is developed, which is in good agreement with the experimental data.

In this paper, a new strengthening technique of prestressed CFRP patched by ractive powder concrete (RPC) pad is developed. To study its performnace and strengthening effects, the axial compression performance of 15 prestressed CFRP reinforced concrete columns pacthed with RPC pads is studied through full scale tests. The effects of level of prestressing force, number of CFRP layers and strenghthening process on the reinforcement effect of the RC columns under different loadings are investiagted. The improvement of the compressive performance of the columns and the failure mechanism are studied. At the same time, the "residual strength" theory is used to develop a formula to caclaucte the axial compressive stength of the RC cloumns , which is validated on the experimental value, accurate predictions are acheived.

2. Test Program

2.1 Casting the the concrete columns

In the study, only short conlumns are investigated. Therefore, the crossection of the columns are 200mm × 200mm and the length is 1000mm. In addition, the dimension of the specimens are chosen with the consideration of the limitation of the loading capacity of the testing machine in the lab.The reinforcement deatils are shown in Figure 1. To prevent the crushing of the concrete at the the loading end, additional steel mesh and the CFRP strips are placed at the end of the column. HPB300 grade steel rebars and mesh are used for stirrups and HRB400 grade steel rebars are used for longitudinal reinforcement. The mechanical properties of reinforcement, RC concrete are shown in Table 1-2. The concrete strength is C30. The CFRP is using CFS-I-300 type unidirectional fiber cloth, and the mechanical properties are shown in Table 3. The pad is divided into two sections: round conner shape pads and rectangular shape pads. The chamfering radius of the round conner is 25mm. The thickness of the pad is 30mm, which is the same thickness as the anchor. Its height is slightly larger than the width of CFRP strips. Table 4 shows the The mechanical properties of the RPC material used.

The test parameters are shown in Table 5,which include applied axial load N_c, design axial load

to section pressure ratio μ_s, actual load level percentage μ_f (is the ratio of the initial axial load N_c to the measured value of the axial capacity of the reference column Z-0), level of prestressed force α (the ratio of the tensile stress of CFRP to its ultimate strength), number of wraps of fiber cloth n, and strenthened process. In Table 5, specimnes Z-0 is unstrengthend,ZD-0031 and ZD -0041 are strengthened using unpadded blocks (chamfering treatment) with a chamfer radius of 25 mm, the remaining are strenthened using this new technique.
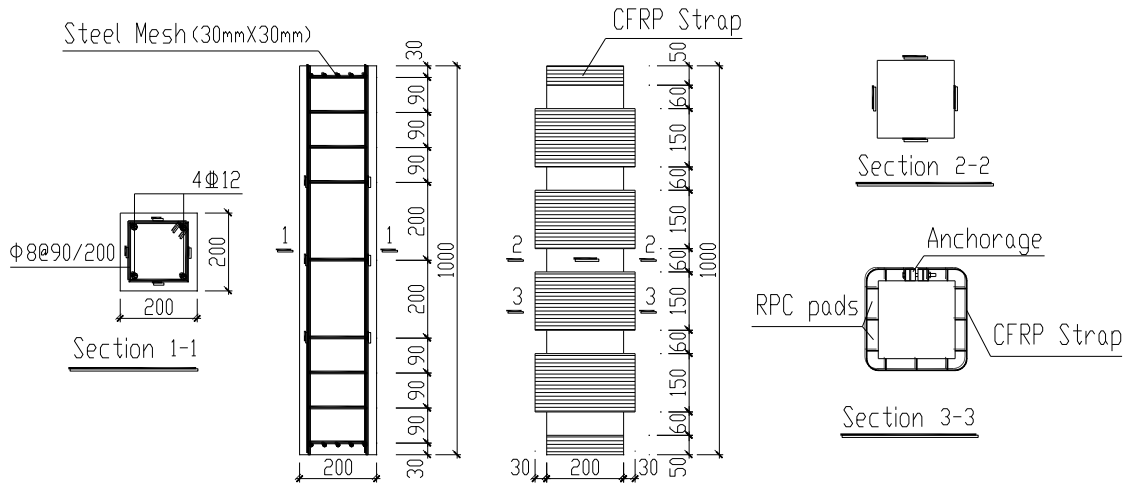

Fig.1 Specimen size, reinforcement, location of the CFRPs and Location of strain gauges for steel and concrete

Table 1 Mechanical properties of reinforcement

Type of Reinforcement	Yield strength f_y /MPa	Ultimate strength f_{st}/MPa	Young's Module E_s/MPa
HPB300	345	475	2.1×10^5
HRB400	435	590	2.0×10^5

Table 2 Mechanical properties of RC concrete

Cube compression strength f_{cu}/MPa	Cylindrical compression stress f_c/MPa	Young's Module E_c/MPa
29.98	21.87	2.98×10^4

Table 3 Mechanical properties of CFRP

Thickness t_f/mm	Tensile strength f_f /MPa	Elongation rate δ_f/%	Young's Module E_f/MPa
0.167	3634	1.65	2.38×10^5

Table 4 Mechanical properties of RPC pads

Cube compression strength	Cylindrical compression stress	Young's Module
f_{cur}/MPa	f_{cr}/MPa	E_{cr}/MPa
127.1	117.2	4.1×10^4

Table 5 Parameters of specimens

Number	N_c/kN	μ_s	μ_f	α	n	Fabrication Process
Z-0	0	0	0	0	0	Unstrengthen
Z-0031	0	0	0	0.3	1	RPC pad
Z-0631	345	0.6	0.39	0.3	1	RPC pad
Z-0831	460	0.8	0.52	0.3	1	RPC pad
Z-1031	575	1.0	0.65	0.3	1	RPC pad
Z-0041	0	0	0	0.4	1	RPC pad
Z-0641	345	0.6	0.39	0.4	1	RPC pad
Z-0841	460	0.8	0.52	0.4	1	RPC pad
Z-1041	575	1.0	0.65	0.4	1	RPC pad
Z-0032	0	0	0	0.3	2	RPC pad
Z-0632	345	0.6	0.39	0.3	2	RPC pad
Z-0832	460	0.8	0.52	0.3	2	RPC pad
Z-1032	575	1.0	0.65	0.3	2	RPC pad
ZD-0031	0	0	0	0.3	1	Chamfer angle
ZD-0041	0	0	0	0.4	1	Chamfer angle

2.2 Prestressed CFRP installation

The anchoring device used for CFRP is the same as used in literature [26], and the thickness of the anchor clip is reduced to be consistent with the thickness of the RPC pad. In order to ensure that

the screws in the anchor not bend and deform when high prestress is applied. The specific steps include: 1. Prefabricated modular RPC pads, including segments of the round column corner blocks and normal rectangular blocks. 2. Glue the prefabricated block using epoxy in the pre-designed strengthening area. To prevent pads from sliding downward due to gravity, the steel angle hoop can be pre-installed at a suitable position. The gap between the blocks is filled with glass glue. The anchors are not exposed but concavely embedded between the two rectangular blocks. 3. After the pad and the column are tightly bonded, as well as the anchor and CFRP are in position, the prestressing force is applied by tightening the high-strength bolt with a wrench. The applied pre-stress level can be controlled by the strain value on the fiber cloth measured at the end of the anchor. The installation diagram is shown in Figure 2. In order to ensure the overall force of the CFRP filaments, the "de-filing phenomenon" due to process or quality problems is prevented to ensure that the pre-stress can be effectively and uniformly transmitted. After the pre-stress is applied, the surface of the cloth is coated with a layer of impregnating glue.
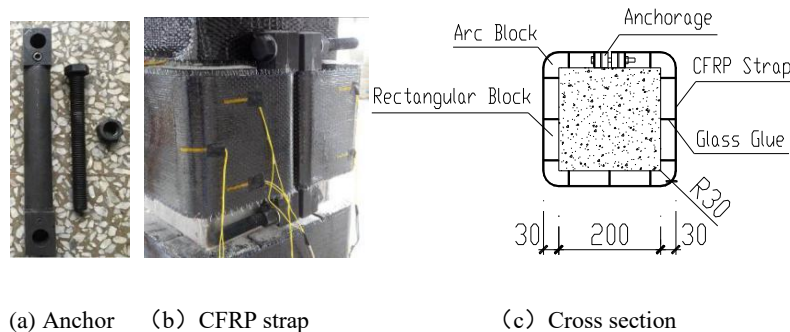

(a) Anchor   （b）CFRP strap   （c）Cross section

Fig.2 Schematic diagram of the anchorage system

2.3 Loading procedure

The compression test machine with a load range of 5000kN is shown in Figure 3. The baseplate of the column is pin supported. The loading is carried out incrementally according to the Standard of Concrete Structure Test Method (GB/T 50152-2012). The specimens were first preload with about 20% of the peak load of the column Z-0 and kept the same load level for 2 min to check the readings of strain gauges of the longitudinal reinforcement and the concrete. The formal loading increment is 40kN with the loading rate of 0.5kN/min. When the load increased to the desired load, the load value is maintained, the strengthening process started. The surface of the fiber cloth is glued with strain gauges. The sheet is prestressed with prestressing value of CFRP kept stable. Then, second loading starts until the longitudinal rebars are about to yield, the load increment reduces to10kN, with loading rate of 0.2kN/min, and each stage is stabilized for 2min after loading. During the test, below parameters are monitored: 1. Load and axial displacement, which can be directly measured by the loadcell and the displacement control system. 2. The strain of the carbon fiber cloth includes the strain at the corner and the middle of the column and ensures that it is bonded to the same fiber filament in the middle of the fiber cloth. 3. The strain of longitudinal reinforcement, stirrup and concrete in the middle of the column.

Fig.3 Test rigs

2.4 Instrumentation

The load is recorded using the built-in load cell in the compression testing machine. The axial displacement is monitored through a displacement transducer which is also built in the testing machine. The strain gauges are glued directly to the same fiber of the CFRP strips as it is shown in Figure 1 and 3. The average readings of the strain gouges are taken as the strain of the CFRP strip. In addition, the strain gauges are also glued to the longitudinal rebars and stirrups to measure the stain changes in the rebars.
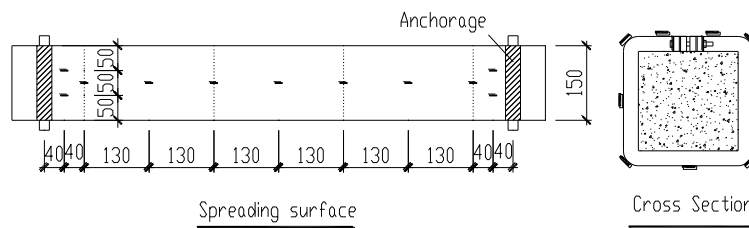

Fig.4 Location of CFRP strain gauges

3. Test results and analysis

3.1 Test observation

Figure 5 shows the failure mode of each specimen. As column Z-0 is not strengthened, there is no obvious change at the initial stage of loading for Z-0. When it was increased   to about 80% of the ultimate load, longitudinal cracks appeared in the upper part of the column. With the increase of the load , the crack extended downward. When it is loaded to 90% of the ultimate load, the crack in the middle and upper corners is obvious, the crack penetrated and concrete covers fell off, the column was destroyed.

The rest specimens are strengthened columns, when the initial axial force applied no crack or damage on the surface of the unreinforced column were noticed. When the load reached 90% of the

ultimate load, at the location of where the column angle is not wrapped, longitudinal crack was noticed in the concrete, longitudinal reinforcement yield, as the prestressing degree increases, the load when the crack first observed increased as well.
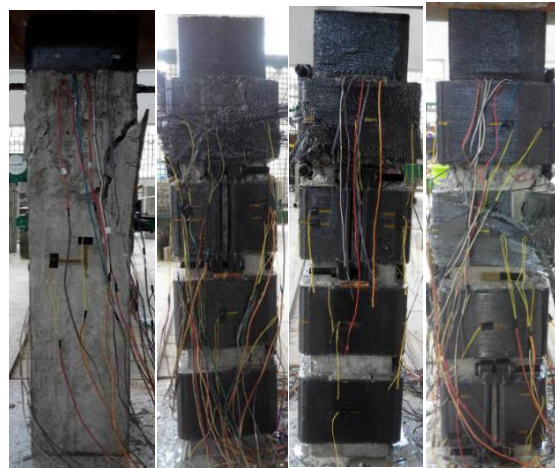
(a) Z-0   (b) Z-0031   (c)Z-0831   (d)Z-0641
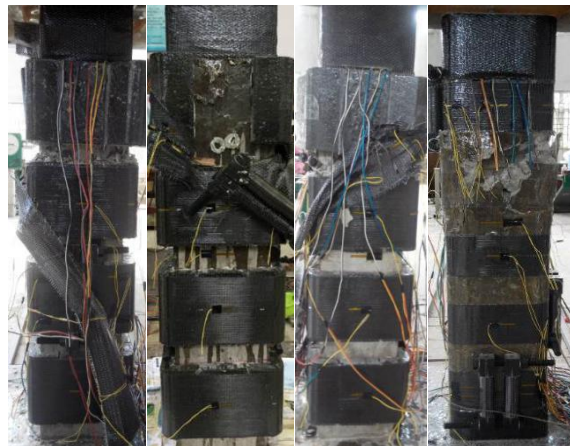
(e)Z-0032   (f)Z-0832   (g)Z-1032   (h)ZD-0041

Fig.5 Failure mode of different specimens

(a)CFRP cloth rupture   (b)Crush of concrete core   (c)RPC patch

Fig.6   Local failure mode

The damage of the reinforcing member began with the fracture of the CFRP cloth when the sound

of the fiber broken was heard. Then the core concrete was crushed. The RPC pad is intact, as shown in Figure 6. It is noticed that the ultimate axial capacity and ductility of the strengthened member are significantly increased compared to column Z-0.

Before the specimens was loaded, there was a small amount of bonding crack at the interface between the concrete coarse aggregate and the cement mortar. For column Z-0, the internal micro-crack began to increase and expand, and gradually developed into a macro-crack. The internal damage of the components accumulated continuously, eventually lost the axial capacity and destroyed. For the strengthened columns, due to strengthening of the prestressed CFRP, an effective hoop constraint force is applied to the concrete. This active restraining force can partially close up some microscopic and macroscopic cracks, delay the development of the crack. The more the wraping area and the number of layers, the more significant the delay effect. When the axial capacity reached the ultimate load, the carbon fiber cloth can no longer restrain the lateral deformation of the concrete, the fiber filament was broken, and the energy accumulated inside the component was suddenly released. Therefore, the confined concrete inside columns was destroyed more than the reference specimen column Z-0 without strengthening.
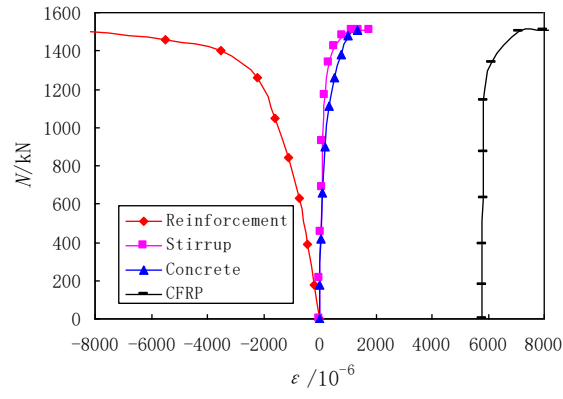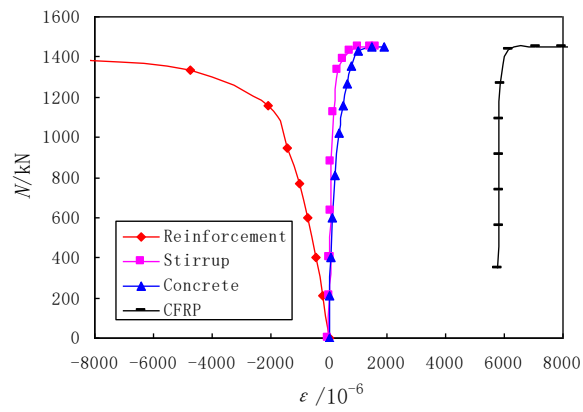
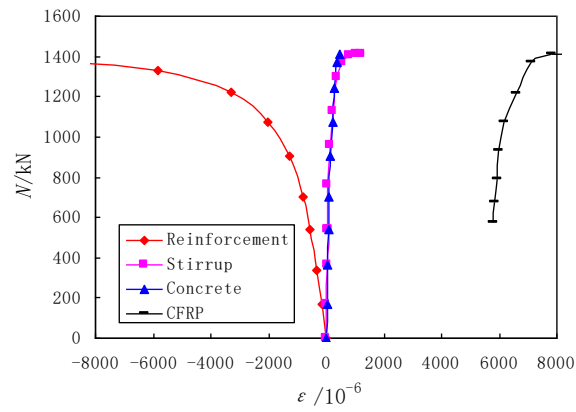### 3.2 Strain guage reading
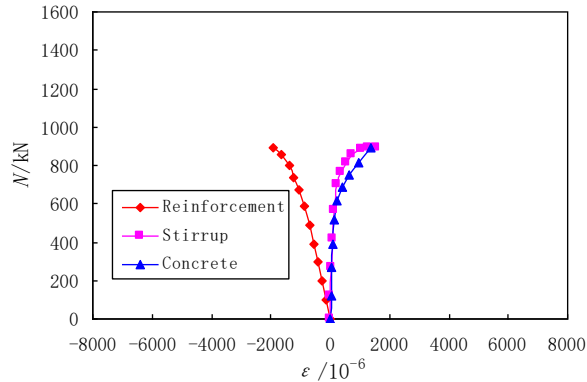
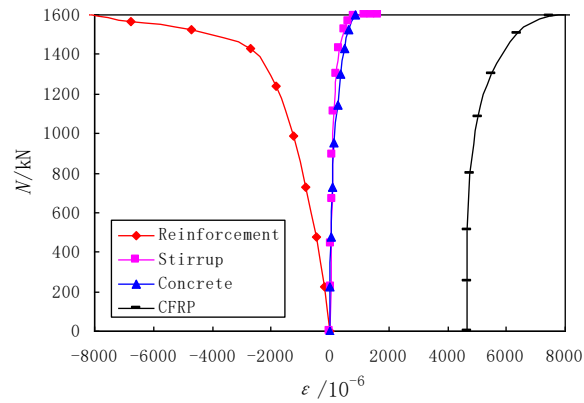(a) Specmen Z-0
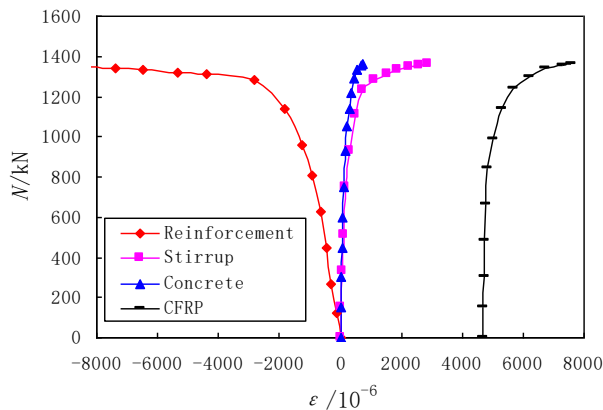
(b) Z-0031

(c) Z-0041

(d) Z-0641

(e) Z-1041

(f) Z-0032

Fig.7 Load-strain relationship of reinforcement, stirrup, concrete and CFRP straps

Figure 7 shows the load-strain relationship curves of for different components for each specimen with different prestressing degrees, load levels, and fiber cloth layers. It can be seen from the figure that, before failure, the longitudinal reinforcement is yielded first (except Z-0), and the plastic deformation is observed. Then the stirrup yields, the carbon fiber cloth reaches the ultimate tensile strain, and the concrete is crushed.

For un-strengthened column Z-0, the strain of the longitudinal reinforcement increased rapidly with the increase of the load. When it reaches $1000\mu\varepsilon$, the concrete strain increased rapidly, and was destroyed, and the crush of the concrete stopped the full development of the deformation of the longitudinal reinforcement.

After strengthening, the slope of the steel bar and concrete strain curve increased obviously, and the inflection point appeared later. The longitudinal reinforcement deformation was fully developed. The stirrups were plastically deformed when the member was close to the failure, indicating the circumference direction was confined by carbon fiber cloth. The strength of steel and concrete materials was fully utilized, and the compression performance of the columns was fully improved. The increase of prestressing level and the number of carbon fiber cloth layers, the better the working performance. Both the Stirrups and concrete different degrees of strain shrinkage, which increases with the increase of the applied prestressing value. For details, see Fig. 8, where $\Delta\varepsilon$ is the strain shrinkage value.
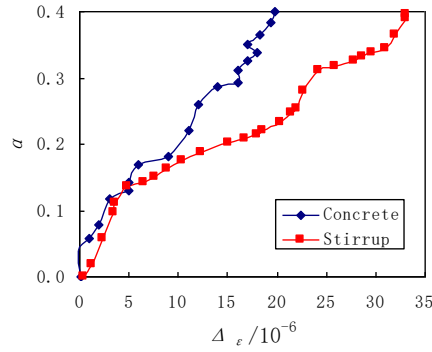
Fig.8 Stirrups and concrete strain shrinkage of Z-1041

3.3 Load and deformation relationship

(a)Specimens with $\mu_s=0$

(b)Specimens with $\alpha=3$ and $n=1$

(c)Specimens with $\alpha=4$ and $n=1$

(d)Specimens with $\alpha=3$ and $n=2$
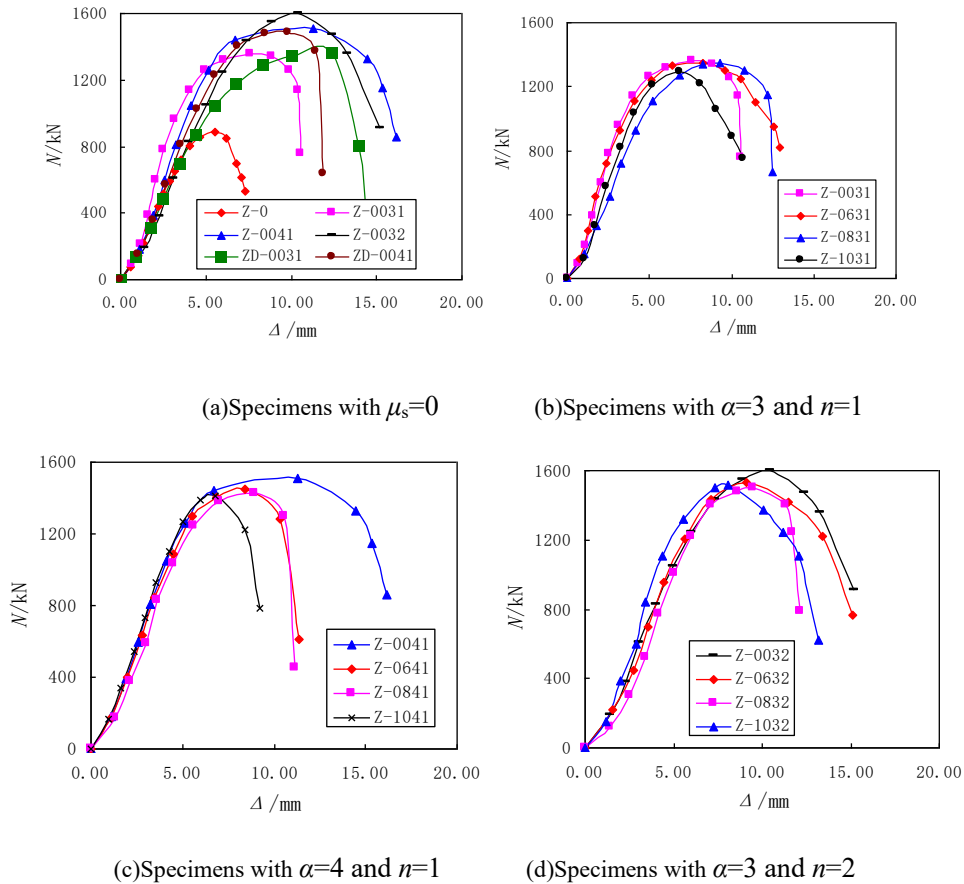
Fig.9 Load-axial displacement relationship

The load-axial displacement curve of each specimens is shown in Fig. 9. In the figure, Δ is the axial displacement. It can be seen from Fig. 9(a) that the ultimate load of the strengthened column decreases in comparison to column Z-0. There is an evident yield plateau for the strengthened columns after peak load, indicating that the ductility of the member is also improved, among which Z-0041 and Z-0032 are most obvious. It shows that the increase of prestressing level and the

number of carbon fiber cloth layers have obvious effects on improving the structural performance of the members. From the comparation between h ZD-0031 and ZD-0041, the RPC pad method and the traditional chamfering method are used respectively, it can be seen that, there is no obvious difference in the strengthening effect, and the ductility of the member is slightly better of the new methods than the chamfer method. Figure 9(b), (c), and (d) are all members with different load levels. The load value has a relatively small influence on the ultimate axial compressive capacity of the reinforcing column, but it has a greater influence on the ductility of the member. The main characteristic points data of the graph of Fig. 9 is shown in Table 6, where N_{ex} is the ultimate load, Δ_u is the displacement corresponding to N_{ex}, Δ_m is the ultimate displacement of the member, and the displacement when the load is lowered to $0.6N_{ex}$ is uniformly taken. γ is the increase percentage of the column axial capacity.

Table 6 test result at main characteristic points

Number of specimens	N_{ex}/kN	γ/%	Δ_u/mm	Δ_m/mm
Z-0	890	0	5.54	7.27
Z-0031	1360	52.8	7.59	10.55
Z-0631	1355	52.2	7.69	12.97
Z-0831	1350	51.7	9.28	12.45
Z-1031	1290	44.9	6.86	10.61
Z-0041	1510	69.7	11.32	16.05
Z-0641	1450	62.9	8.42	11.05
Z-0841	1430	60.7	8.93	10.94
Z-1041	1410	58.4	6.81	9.10
Z-0032	1600	79.8	10.41	15.01
Z-0632	1530	71.9	9.11	14.59
Z-0832	1500	68.5	9.48	12.09
Z-1032	1520	70.8	8.04	12.56
ZD-0031	1363	53.1	12.39	13.90
ZD-0041	1490	67.4	9.85	11.77

From table 6, it can be seen that the axial capacity and ductility of all strengthened columns are improved compared with those of un-strengthened columns. This is because the pre-stressed CFRP restricts the development of column cracks. Even if there are any initial micro cracks, due to the wrapping of the pre-stressed CFRP, some cracks closed. Therefore, the stiffness of the reinforced

columns is maintained in a better condition during the whole loading process. The ultimate load of the component increases with the increase of the prestressing force and the number of CFRP layers, and the influence of the number of CFRP layers is greater than that of the prestressing force. The ductility of members is also increased with the increase of prestressing force and reinforcement layers, and the influence of reinforcement layers on ductility is more obvious, especially under load. The specimen z-0032 is the best in terms of its performance, wrapped by a double layer cloth with a prestressing force of 0.3, which is also the ultimate prestress force the CFRP anchor device can exert.

4. Analytical model for the axial strength of confined concrete

4.1 Basic assumptions

It can be seen from the test phenomenon that the failure modes of the member are: fiber cloth broken or peeled off, inner core concrete crushed. This indicates that the fiber cloth can fully develop its high strength due to the prestressing. In the meantime, the core concrete is under triaxial compression state, the strength is increased more than when it is under uniaxial compression. The following assumptions are made in the calculation : 1. The cross-section is always in the same plane during the compression process; 2. The CFRP does not resist the axial load to the column and only resist the tensile stress in the circumferential direction; 3. CFRP and RPC pad have good contact with the concrete surface, and no relative slip. 4. Because the distance between the stirrups is large, their restraining effect on the core concrete is neglected, which is provided only be CFRP.

4.2 Axial strength of un-loaded strengthened concrete

4.2.1 Existing analytical model

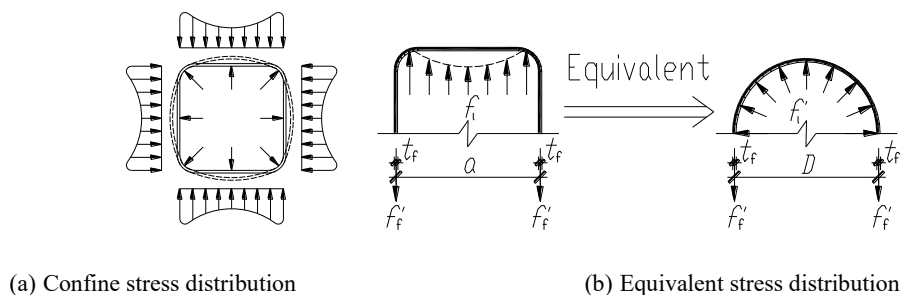(a) Confine stress distribution   (b) Equivalent stress distribution

Fig.10 Confine stress distribution and equivalent simplification

When the column is subjected to axial compression, the concrete will expand along the radius, and the radial deformation will be greatly limited by the restraint from prestressed CFRP. The confined concrete is in a high triaxial compression state, and its strength has been greatly improved. For circular section columns, the strengthening effect relies primarily on maximum restraint provided by prestressed CFRP and the CFRP layers, degree of prestress and diameter of column section.

Since the column section is square, the constraint from the corner fiber cloth results a resultant force along the 45° diagonal direction in the core concrete, and at the same time, the fiber cloth on the

side surface bulges due to the lateral expansion of the concrete, thereby, reducing the restraining effect. Therefore, the circumferential stress distribution of the fiber cloth is not uniform, and the restraining effect on the core concrete is large at the corner portion and small in the middle, as shown in Fig. 10(a). In Fig. 10, f_l is the constraint stress of the square section, f_l' is the constraint stress provided by the same thickness of the fiber cloth to the circular section of the equivalent diameter D, f_f' is the ultimate tensile strength of the CFRP ring.

A section shape factor k_s, $k_s = A_e / A$, A_e is the effective constraint area, and A is the total area, which is equivalent to the constraint stress provided by the circular section of diameter D, as shown in Fig. 10(b) is introduced by Mirmiran [27]. Considered that D is equal to the side length of the square section a, Lam et al. [22] developed the calculation model of axial compression strength f_{cc} of the CFRPs restraint square column concrete is proposed. Formula 1:

$$\frac{f_{cc}}{f_c} = 1 + k_1 k_s \frac{f_l'}{f_c} \qquad (1)$$

Where: f_c The compressive strength of the confined concrete can be measured by the test. k_1 is an effective constraint coefficient and can be obtained by regression.
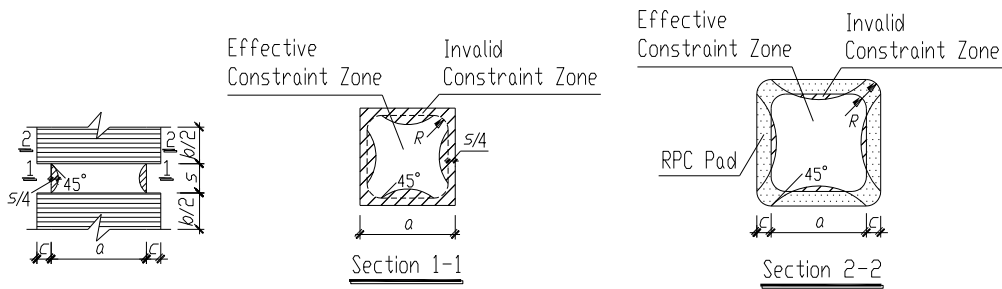
4.2.2 Determine section shape factor k_s

Fig.11 Effective constraint area

The patching method of the CFRP cloth in this test is discontinuous e, taking a representative calculation unit along the column height, as shown in Figure 11, b is the package width, s is the package pitch, c is the pad thickness, and R is the pad chamfer radius. The 1-1 section is the midpoint section of the unwrapped portion, the 2-2 section is the section of the package, and the unfilled area on the section is the effective constraint zone, as shown in the figure, for the 1-1 section:

$$k_{s1} = \frac{A_{e1}}{A_1} = 1 - \frac{2}{3}(1 - \frac{s}{2a} - \frac{2R}{a})^2 \qquad (2)$$

For section 2-2：

$$k_{s2} = \frac{A_{e2}}{A_2} = 1 + \frac{4c}{a} - 4(\frac{c}{a})^2 - \frac{2}{3}(1 + \frac{2c}{a} - \frac{2R}{a})^2 \quad (3)$$

For the equilibrium of lateral force acting on the column, the weighted average of k_{s1} and k_{s2} along the height can be worked out as (4);

$$k_s = \frac{k_{s1}s + k_{s2}b}{s+b} \quad (4)$$

4.2.3 Determine the lateral restraint force f_l'

Since the distance between the fiber cloths of the test is relatively dense, b is much larger than s, to be conservative, a representative free body along the direction of the column length which is not unconstrained is taken. Considering the equivalent simplification of show in Figure 9(b), the forces balance is available:

$$2f_f' nt_f b = f_l'(ab + as - s^2/2) \quad (5)$$

Since the ultimate tensile stress of the circumferentially stretched fiber cloth is lower than that under direct tension, that is, $f_f' < f_f$ according to the measured value of the fiber cloth strain corresponding to the ultimate bearing capacity of the member in the test, the effective tensile strain coefficient of the fiber cloth is introduced in this paper, as shown in Table 6, that is $\eta = \varepsilon_f'/\varepsilon_f = f_f'/f_f$, ε_f 、 ε_f are the measured values of the fiber cloth strain corresponding to the the ultimate tensile strain under the straight tension, representing the effective utilization of carbon fiber cloth when the component is broken. It can be seen from the test that the main factors affecting η are the degree of prestress, the number of layers of fiber cloth and the construction process.

Table 6 Effective strain coefficient

Number of specimens	ε_f' /10^{-6}	ε_f /10^{-6}	η
Z-0031	8524	15269	0.56

Z-0631	7676	15269	0.50
Z-0831	9039	15269	0.59
Z-1031	9069	15269	0.59
Z-0041	8905	15269	0.58
Z-0641	8677	15269	0.57
Z-0841	8487	15269	0.56
Z-1041	9614	15269	0.63
Z-0032	8905	15269	0.58
Z-0632	7048	15269	0.46
Z-0832	7065	15269	0.46
Z-1032	8422	15269	0.55

4.3 Formula to calculate the confined concrete under load

From the residual strength theory [23-25], The the CFRP can only increase the residual axial stress of the core concrete, but no effect on the innitial stress of developed in the un-strengthed concrete,Therefore, the calculation of the axial compressive strength of confined concrete under load can be divided into two stages: the first stage is the calculation of the compressive stress level of the unconstrained concrete under the initial load; the second stage is the prestressing due to the fiber cloth restrains. The final axial capacity of the column is the force superposition of the two-stage calculation.

Stage 1: assuming that the compressive stress of the concrete under the initial load is σ_0 , the

residual compressive strength at the time of un-strengthened concrete $f_{c,rem}$ is:

$$f_{c,rem} = f_c - \sigma_0 = f_c - N_c / A \qquad (6)$$

Stage 2　It is assumed that the concrete with residual compressive strength is regarded as concrete having the same compressive strength without initial compressive stress level, and the strength of the residual concrete after the compressive strength is increased $f_{cc,rem}$ is:

$$\frac{f_{cc,rem}}{f_{c,rem}} = 1 + k_1 k_s \frac{f_l'}{f_{c,rem}} \tag{7}$$

The compressive strength of the confined concrete under the final load is a two-stage stress superposition, see equation (8).

$$f_{cc} = f_{c,rem} + \sigma_0 \tag{8}$$

4.4 Regression of effective confinement coefficient k_1

It is known from the literature [22] that the effective constraint coefficient k_1 is a variable, therefore, the regression analysis is needed based on the experimental data. The relevant data of equations (6) and (7) are listed in Table 7, where σ_0、$f_{c,rem}$ can be obtained from the tests. k_s、f_l' can be obtained can be obtained from equations (4) and (5), respectively.

Table 7 Regression parameters

Number	σ_0/MPa	$f_{c,rem}$/MPa	$f_{cc,rem}$/MPa	k_s	f'_l/MPa
Z-0031	0	21.87	34.00	0.77	2.32
Z-0631	8.63	13.24	25.25	0.77	2.07
Z-0831	11.50	10.37	22.25	0.77	2.45
Z-1031	14.38	7.49	17.88	0.77	2.45
Z-0041	0	21.87	37.75	0.77	2.41
Z-0641	8.63	13.24	27.63	0.77	2.36
Z-0841	11.50	10.37	24.25	0.77	2.32
Z-1041	14.38	7.49	20.88	0.77	2.61
Z-0032	0	21.87	40.00	0.77	4.81
Z-0632	8.63	13.24	29.63	0.77	3.82
Z-0832	11.50	10.37	26.00	0.77	3.82
Z-1032	14.38	7.49	23.63	0.77	4.56

According to the regression parameters in Table 7, the relation between $f_{cc,rem}/f_{c,rem}$- $k_s f'_l/f_{c,rem}$ can be worked out from Figure 12, the relation can be expressed as：

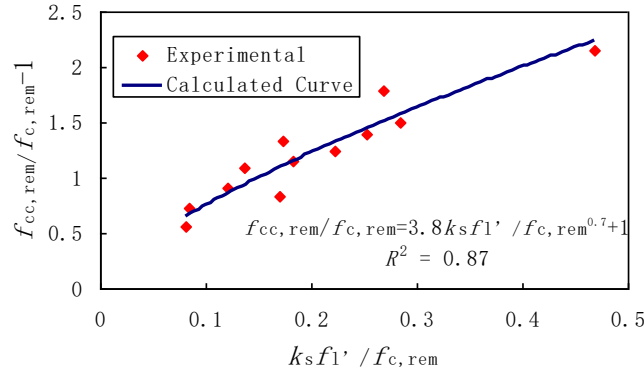$$\frac{f_{cc,rem}}{f_{c,rem}} = 1 + 2.9(\frac{f_l'}{f_{c,rem}})^{0.7} \qquad (9)$$

Fig.12 Relationship of $f_{cc,rem}/f_{c,rem}$- $k_s f_l'/f_{c,rem}$

5. Analytical model to calculate the axial compressive capacity of the RC columns

5.1 Basic Assumptions

In order to simplify the calculation, the following assumptions are made: (1) the axial load is mainly resisted by the longitudinal reinforcement and the concrete, and the CFRP sheet does not resist the axial load; (2) there is no relative slip between the CFRP sheet and the concrete surface, and the deformation between them is compatible ; (3) The deformation of concrete in the effective constraint area and the non-effective constraint area is also compatible; (4) when calculating the axial compressive capacity of concrete, the ultimate compressive strength of confined concrete is used.

5.2 Calculation formula for the RC columns

According to formula 8, the compressive strength of confined concrete column under load can be developed based on residual strength theory, and the axial compressive capacity of reinforced column can also be calculated in two stages: the first stage is before strengthening, and the axial capacity at this stage is not improved. The second stage is the capacity of the column after strengthening, the column continues to resist extra load due to the increase of the residual compressive strength of the concrete under the condition of prestressed fiber cloth constraint. At the same time, the strengthening only affects the concrete but the longitudinal reinforcement, that is, the compressive bearing capacity provided by the longitudinal reinforcement does not change before and after the strengthening.

As the scope of this study is on short columns, the effect of the slendeness and accidental eccentricity of the columns can be ignored, the ultimate axial compressive capcity N_u has 3 components: innitial comression capcity of concrete N_c、 axial capcity from the reinforcement $N_{s,rem}$, Axial capcity from confied concrete $N_{cc,rem}$， So：

$$N_u = N_c + N_{s,rem} + N_{cc,rem} \qquad (10)$$

And $N_{s,rem} = f_y A_s (1 - \mu_f)$, $N_{cc,rem} = f_{cc,rem} A_c$, Where A_s is cross section area of steel，A_c is the area of the concrete, and $A_s + A_c = A$。

5.3 Formula validation

The above formula is validated against test results, the validation results are show in Table 8, it can be seen that, good agreemet is acheived.

Table 8 Comparison of calculated and test value of axial compression capacity

Number of Specimens	$N_{s,rem}$/kN	$N_{cc,rem}$/kN	N_u/kN	N_u/ N_{ex}
Z-0031	197	1187	1384	1.02
Z-0631	120	817	1282	0.95
Z-0831	95	747	1302	0.96
Z-1031	69	619	1263	0.97
Z-0041	197	1202	1399	0.93
Z-0641	120	857	1322	0.91
Z-0841	95	731	1286	0.89
Z-1041	69	637	1281	0.91
Z-0032	197	1535	1732	1.08
Z-0632	120	1038	1503	0.98
Z-0832	95	905	1460	0.97
Z-1032	69	833	1477	0.97
Mean				0.96
Standard Deviation				0.05

6 Conclusions

In this paper, a new type of prestressed CFRP strengthening technique using RPC pads was developed. The performance of the columns strengthened by this new technique was tested through a series of compression tests. Based on the test results and the residual strength theory, an analytical model to calculate the axial compressive capacity of the columns strengthened using this new

technique is developed. Below conclusions can be made

1. Compared with the traditional chamfering method, this new method can provide rapid strengthening solution during the construction process, it reduces the dust pollution caused by the column angle grinding, however, the strengthening effect is not significantly different to the traditional method.

2. The ductility is slightly better than those using the chamfering method, at failure , the RPC pads are intact, indicating that the material can serve well as a medium for transmitting the binding force from prestressed CFRP.

3. Increasing the degree of prestress level and CFRP layer within a certain range can improve the axial bearing capacity of the component (up to 80%) and improve the structural performance of the component under normal use conditions. However, due to the feature of CFRP cloth, attention should be paid to the influence of construction disturbance when high prestress is applied;

4. The strength calculation model of confined concrete based on the "residual strength" theory can accurately predict the axial capacity of concrete square columns strengthened by this new technique.

References

[1]. GUO Zixiong, HUANG Qunxian, YANG Liu, et al. Review on the research of RC columns strengthened with transverse prestressed steel sheath[J]．Engineering Mechanics, 2016, 33(3): 1-9.

[2]. ZHANG Bo, YANG Yong, LIU Yi, et al. Experimental study on axial compression behavior of reinforced concrete columns strengthened with prestressed steel strips．Engineering Mechanics, 2016(03): 104-111.

[3]. LAM S S E, WANG Z Y, LIU Z Q, et al. Drift Capacity of Rectangular Reinforced Concrete Columns with Low Lateral Confinement and High-axial Load. Journal of Structural Engineering, 2003, 129(6):733-742.

[4]. YE Lieping, FENG Peng . Applications and development of fiber-reinforced polymer in engineering structures. China Civil Engineering Journal, 2006, 39(3): 24-36.

[5]. TSONOS A G. Effectiveness of CFRP-jackets and RC jackets in post-earthquake and pre-earthquake retrofitting of beam-column subassemblages. Engineering Structures, 2008, 30(3) 777-793.

[6]. BENZAID R, CHIKH N E, MESBAH H. Behaviour of square concrete column confined with GFRP composite warp. Journal of Civil Engineering and Management, 2008, 14(2): 115-120.

[7]. BOUSSELHAM A. State of research on seismic retrofit of RC beam-column joints with externally bonded FRP. Journal of Composites for Construction, 2010, 14(1) : 49-61.

[8]. MOSTOFINEJAD D, SAADATMAND H. A procedure for predicting the behavior of FRP confined concrete using the FE method [J]. Sci Iran Trans A Civil Eng, 2010, 17(6): 471-481.

[9]. CECS146-2003 Technical specification for strengthening concrete structure with carbon fiber reinforced polymer laminate. Beijing: China Planning Press, 2003.

[10]. JING Denghu, CAO Shuangyan. A model for calculation the axial stress-strain curve of square-section concrete column confined by FRP . China Civil Engineering Journal, 2005, 38(12): 32-37 .

[11]. LIU Tao, FENG Wei, ZHANG Zhimei, et al. A study on the compressive performance of rectangular concrete columns confined with CFRP sheets . China Civil Engineering Journal, 2006, 39(12): 41-47 .

[12]. WANG Jizhong , WANG Suyan, HUANG Chengkui. Research on ductility and earthquake-resistance of high-strength concrete column confined by CFRP . Journal of Dalian University of Technology, 2008,48(5):708-714.

[13]. WEI H, WU Z, GUO X, et al. Experimental study on partially deteriorated strength concrete columns confined with CFRP, Engineering Structures, 2009, 31:2495-2505.

[14]. MOSTOFINEJAD D, MOSHIRI N, MORTAZAVI N. Effect of corner radius and aspect ratio on compressive behavior of rectangular concrete columns confined with CFRP. Materials and Structures, 2013, 48(1-2): 1-16.

[15]. HAO Haixia, ZHANG Jianren, GAO Yong, et al. Simplified analysis on bond performance of near-surface mounted CFRP-concrete interface. Chinese Journal of Highway and Transport, 2015,28(4):52-59.

[16]. Masoud Motavalli ,Christoph Czaderski Kerstin Pfyl-Lang, Prestressed CFRP for Strengthening of Reinforced Concrete Structures: Recent Developments at Empa, Switzerland, J. Composite Construction, 2011, 15(2): 194-205

[17]. Elyas Ghafoor, Ardalan Hosseini, Riadh Al-Mahaidi, Xiao-Ling Zhao, Masoud Motavalli, Prestressed CFRP-strengthening and long-term wireless monitoring of an old roadway metallic bridge, Engineering Structures, Volume 176, 1 December 2018, Pages 585-605

[18]. ZHOU Changdong, LI Ji, LV Xilin. Experimental research on pre-stress loss of concrete circular columns confined with posted-tensioned FRP. Journal of Tongji University(Natural Science). 2012, 40(12): 1760-1765.

[19]. ZHOU Changdong, BAI Xiaobin, ZHAO Feng, et al. Experimental study on axial compressive behavior of concrete short columns strengthened with prestressed CFRP sheets, Journal of Building Structures, 2013, 34(2): 131-140.

[20]. RICHARD P, CHEYREZY M．Composition of reactive powder concretes, Cement and Concrete Research, 1995, 25(7):1501-1511.

[21]. Mander J. B，Priestley M. J. N.and Park R.(1988) "Theoretical stress-strain model for confined concrete", Journal of Structural Engineering, ASCE, 1988, 114(8): 1804-1826.

[22]. LAM L, TENG J G. Strength models for fiber-reinforced plastic-confined concrete. Journal of Structural Engineering, ASCE, 2002, 128(5): 612-623.

[23]. Zhao H. B. Test Study on Mechanical Performance of High-strengthConcrete Column Confined by CFRP under Axial Load. Dalian University of Technology，2006.

[24].Huang J. Experimental Study And Simul Ation on Compressive Behavior Of Preloaded Strengthened Concrete Columns with GFRP. Dalian University of Technology，2005.

[25].PAN Congjian. Experiment study on the compressive behavior of circular concrete columns confined with FRP considering the secondary load . China Academy of Building Research, 2007.

[26].ZHOU Changlong, LI Ji, ZHU Wanxu, et al. Design of self-locking anchor system of FRP and research on mechanical properties, Journal of Building Structures, 2013, 34(2): 141-148.

[27].MIRMIRAN A, SHAHAWY M, SAMAAN M, et al. Effect of column parameters on FRP-concrete. Journal of Structural Engineering, ASCE, 1998, 2(4): 175-185.